

THE CONTINUOUS SPECTRUM OF THE SUN AND THE STARS

S. CHANDRASEKHAR AND GUIDO MÜNCH¹

Yerkes Observatory

Received September 5, 1946

Using the recent determination of the continuous absorption coefficient of H^- by Chandrasekhar and Breen, we have shown that the dependence of the continuous absorption coefficient with wave length in the range 4000–24,000 Å, which can be inferred from the intensity distribution in the continuous spectrum of the sun, can be quantitatively accounted for as due to H^- ; and, further, that the color temperatures measured in the wave-length intervals 4100–6500 Å (Greenwich) and 4000–4600 Å (Barbier and Chalonge) for stars of the main sequence and of spectral types A0–G0 can also be interpreted in terms of the continuous absorption of H^- and neutral hydrogen atoms.

The problem of the discontinuities at the head of the Balmer and the Paschen series is also briefly considered on the revised physical theory of the continuous absorption coefficient.

1. *Introduction.*—The two principal problems in the theory of the continuous spectrum of the stars are, first, to identify the source of the continuous absorption in the solar atmosphere which will account for the intensity distribution in the continuous spectrum of the sun and the law of darkening in the different wave lengths and, second, to account for the observed relations between the color and the effective temperatures of the stars. In this paper we shall show that the major aspects of these two problems find their natural solution in terms of the continuous absorption coefficient of the negative hydrogen ion as recently determined by Chandrasekhar and Breen.² More particularly, we shall show that the dependence of the continuous absorption coefficient with wave length in the range 4000–24,000 Å, which can be deduced from the solar data, can be quantitatively accounted for as due to H^- ; and, further, that the color temperatures measured in the wave-length intervals 4100–6500 Å (Greenwich³) and 4000–4600 Å (Barbier and Chalonge⁴) for stars of the main sequence and of spectral types A0–G0 can also be interpreted in terms of the continuous absorption of H^- and neutral hydrogen.

In addition to the two problems we have mentioned, we shall also consider some related questions concerning the discontinuities at the head of the Balmer and the Paschen series.

2. *The mean absorption coefficients of H^- and H.*—As is well known, the character of the emergent continuous radiation from a stellar atmosphere is determined in terms of the temperature distribution in the atmosphere; and, as has recently been shown,⁵ the temperature distribution in a nongray atmosphere will be given approximately by a formula of the standard type

$$T^4 = \frac{3}{4} T_e^4 (\tau + q[\tau]), \quad (1)$$

where T_e denotes the effective temperature and $q(\tau)$ a certain monotonic increasing function of the optical depth τ , provided that the mean absorption coefficient κ , in terms of which τ is measured, is defined as a straight average of the monochromatic absorptior coefficient weighted according to the net flux $F_\nu^{(1)}$ of radiation of frequency ν in a gray

¹ Fellow of the John Simon Guggenheim Memorial Foundation at the Yerkes Observatory.

² *Ap. J.*, **104**, 430, 1946.

³ Sir Frank Dyson, *Observations of Color-Temperatures of Stars, 1926–1932*, London, 1932; also *M.N.* **100**, 189, 1940.

⁴ *Ann. d'ap.*, **4**, 30, Table 4, 1941.

⁵ S. Chandrasekhar, *Ap. J.*, **101**, 328, 1945. This paper will be referred to as “Radiative Equilibrium VII.”

atmosphere and if, further, $\kappa_\nu/\bar{\kappa}$ is independent of depth. On this approximation, then, the emergent intensity in a given frequency and in a given direction will depend not only on the continuous absorption coefficient at the frequency under consideration but also on the mean absorption coefficient κ over all frequencies.

As the discussion in this paper will establish for the stellar atmospheres considered, the contributions to κ in the visible and the infrared regions of the spectrum are essentially from only two sources: H^- and the neutral hydrogen atoms. The cross-sections for the absorption by H^- for various temperatures and wave lengths have been tabulated by Chandrasekhar and Breen in Table 7 of their paper, while those for hydrogen can be found from the formulae of Kramers and Gaunt, standardized, for example, by B. Strömgren.⁶ However, the evaluation of the mean absorption coefficient for wave lengths shorter than 4000 Å is made uncertain on two accounts: First, there is the absorption by the metals and the excessive crowding of the absorption lines toward the violet, which is particularly serious for spectral types later than F0; and, second, there is the absorption in the Lyman continuum. On both these accounts the true values of $\bar{\kappa}$ will be larger than those determined by ignoring them. But the exact amount by which they will be larger will be difficult to predict without a detailed theory of "blanketing,"⁷ on the one hand, and without going into a more exact theory⁸ of radiative transfer than represented by the approximations leading to equation (1), on the other. However, since in this paper our primary object is to establish only the adequacy of H^- as the source of absorption in the solar atmosphere over the entire visible and infrared regions of the spectrum and the corresponding role of H^- and H for stellar atmospheres with spectral types A2–G0, it appeared best to ignore the refinements indicated and simply determine κ by weighting κ_ν due to H^- and H (without the Lyman absorption) at the conditions prevailing at $\tau = 0.6$ by the flux $F_\nu^{(1)}$ at this level.⁹ For only in this way can we use the solution to the transfer problem in the form of equation (1) in a consistent manner. It should, however, be remembered that the effects we have ignored may easily increase $\bar{\kappa}$, determined in terms of H^- and H (without the absorption in the Lyman continuum) by factors of the order of 1.5 and probably not exceeding 2.¹⁰

Turning our attention, next, to the evaluation of $\bar{\kappa}$, we may first observe that, since our present method of averaging is a straight one, the contributions to κ_ν from different sources are simply additive. We may, accordingly, consider the mean absorption coefficient of H^- and H separately.

Now the absorption coefficient of H^- , including both the bound-free and the free-free transitions, is most conveniently expressed as per neutral hydrogen atom and per unit electron pressure in the unit cm^4/dyne . The monochromatic coefficients κ'_ν , after allowing for the stimulated emission factor $(1 - e^{-h\nu/kT})$, are tabulated in Chandrasekhar and Breen's paper for various values of $\theta (= 5040/T)$. If we now denote by $a(H^-)$ the average

⁶ "Tables of Model Stellar Atmospheres," *Publ. mind. Meddel. Kobenhavns Obs.*, No. 138, 1944.

⁷ Cf. G. Münch, *Ap. J.*, **104**, 87, 1946.

⁸ Such as, e.g., the (2, 2) approximation given in "Radiative Equilibrium VII," § 6.

⁹ The choice of $\tau = 0.6$ for the "representative point" was made after some preliminary trials (cf. G. Münch, *Ap. J.*, **102**, 385, 1945, esp. Table 3), though it is evident on general grounds that a level such as $\tau = 0.6$, where the local temperature is approximately the same as the effective temperature, would be the correct one in the scheme of approximations leading to eq. (1).

¹⁰ In all earlier evaluations of $\bar{\kappa}$ the absorption in the Lyman continuum did not, indeed, play any role. This was due to the manner in which $\bar{\kappa}$ was defined in those investigations as the Rosseland mean. But in "Radiative Equilibrium VII" it has been shown that there is no justification for taking the Rosseland means as they have been hitherto. Since the method of averaging, by which we have now replaced the Rosseland mean, is a straight one, it is no longer permissible simply to ignore the absorption in the Lyman continuum. At the same time, it is not possible to take it into account satisfactorily in the (2, 1) approximation leading to eq. (1). We should have to go at least to the (2, 2) approximation of "Radiative Equilibrium VII."

value of the coefficients κ'_ν , weighted according to the flux $F_\nu^{(1)}$ in a gray atmosphere at $\tau = 0.6$, where the temperature is approximately the effective temperature T_e , then the contribution $\bar{\kappa}(H^-)$ to the mass absorption coefficient $\bar{\kappa}$ by H^- is given by

$$\bar{\kappa}(H^-) = \frac{(1 - x_H) p_e}{m_H} a(H^-), \quad (2)$$

where m_H is the mass of the hydrogen atom, p_e the electron pressure, and x_H the degree of ionization of hydrogen under the physical conditions represented by T_e and p_e .¹¹ The values of $a(H^-)$ found by graphical integration in accordance with the formula

$$a(H^-) = \frac{1}{F} \int_0^\infty \kappa'_\nu F_\nu^{(1)}(0.6) d\nu \quad (3)$$

for various values of $\theta = \theta_e$ are given in Table 1.

TABLE 1
THE MEAN ABSORPTION COEFFICIENTS $a(H^-)$ AND $a(H)$

θ	$a(H^-)$	$a(H)$	θ	$a(H^-)$	$a(H)$
0.5.....	0.563×10^{-26}	1.65×10^{-22}	0.9.....	6.08×10^{-26}	5.52×10^{-27}
0.6.....	1.145×10^{-26}	1.22×10^{-23}	1.0.....	9.32×10^{-26}	3.65×10^{-28}
0.7.....	2.25×10^{-26}	1.13×10^{-24}	1.2.....	2.00×10^{-25}
0.8.....	3.88×10^{-26}	8.00×10^{-26}	1.4.....	3.89×10^{-25}

Similarly, the contribution to $\bar{\kappa}$ by hydrogen can also be expressed in the form

$$\bar{\kappa}(H) = \frac{1 - x_H}{m_H} a(H), \quad (4)$$

where

$$a(H) = \int_0^\infty \frac{fD}{\alpha^3} (1 - e^{-\alpha}) \frac{F_\alpha^{(1)}(0.6)}{F} d\alpha, \quad (5)$$

where $\alpha = h\nu/kT_e$ and f and D are certain functions of temperature and frequency, respectively, which have been tabulated by Strömgen.¹² For reasons which we have already explained, we do not include the Lyman absorption in evaluating $a(H)$. The values of $a(H)$ for various temperatures are also listed in Table 1.

In terms of $a(H^-)$ and $a(H)$ given in Table 1, we can determine the combined mass absorption coefficient $\bar{\kappa}$ according to

$$\bar{\kappa} = \frac{1 - x_H}{m_H} [a(H^-) p_e + a(H)]. \quad (6)$$

Values of $\bar{\kappa}(H^-)$, $\bar{\kappa}(H)$, and $\bar{\kappa}$ determined in accordance with the foregoing equations for various temperatures and electron pressures are given in Table 2.

3. *The continuous absorption in the solar atmosphere*—As we have already stated in the introduction, one of the principal problems in the interpretation of the solar spectrum is the identification of the source of absorption which will predict the same dependence

¹¹ It will be noted that, in writing the mass absorption coefficient in the form (2), we have assumed the preponderant abundance of hydrogen in the stellar atmosphere.

¹² See the reference quoted in n. 6.

of the absorption coefficient with wave length in the range 4000–24,000 Å, which can be inferred from the intensity distribution in the continuous spectrum and the law of darkening in the different wave lengths. While the amount and variation of the continuous absorption in the spectral region $\lambda\lambda$ 4000–24,000 Å can be deduced in a variety of ways,¹³ it appears that, for the purposes of the identification of the physical source of absorption, it is most direct to adopt the following procedure:

TABLE 2
THE MEAN MASS ABSORPTION COEFFICIENTS $\bar{\kappa}(H^-)$, $\bar{\kappa}(H)$, AND $\bar{\kappa}$ FOR VARIOUS TEMPERATURES AND ELECTRON PRESSURES

		$p_e=1$	$p_e=10$	$p_e=10^2$	$p_e=10^3$	$p_e=10^4$
$\theta_e=0.5$	$\bar{\kappa}(H^-)$	5.85×10^{-6}	3.70×10^{-4}	4.98×10^{-2}	2.12	32.1
	$\bar{\kappa}(H)$	1.71×10^{-1}	1.08	14.5	61.8	93.5
	$\bar{\kappa}$	1.71×10^{-1}	1.08	14.6	63.9	126
$\theta_e=0.6$	$\bar{\kappa}(H^-)$	3.93×10^{-4}	2.60×10^{-2}	5.82×10^{-1}	6.68	68.4
	$\bar{\kappa}(H)$	4.18×10^{-1}	2.76	6.19	7.10	7.27
	$\bar{\kappa}$	4.18×10^{-1}	2.79	6.77	13.8	75.7
$\theta_e=0.7$	$\bar{\kappa}(H^-)$	9.08×10^{-3}	1.28×10^{-1}	1.34	13.4	134
	$\bar{\kappa}(H)$	4.54×10^{-1}	6.41×10^{-1}	0.67	0.7	1
	$\bar{\kappa}$	4.63×10^{-1}	7.69×10^{-1}	2.01	14.1	135
$\theta_e=0.8$	$\bar{\kappa}(H^-)$	2.26×10^{-2}	2.32×10^{-1}	2.32	23.2	232
	$\bar{\kappa}(H)$	4.66×10^{-2}	0.48×10^{-1}	0.05
	$\bar{\kappa}$	6.92×10^{-2}	2.80×10^{-1}	2.37	23.2	232
$\theta_e=0.9$	$\bar{\kappa}(H^-)$	3.63×10^{-2}	3.63×10^{-1}	3.63	36.3	363
	$\bar{\kappa}(H)$	0.33×10^{-2}	0.03×10^{-1}
	$\bar{\kappa}$	3.96×10^{-2}	3.66×10^{-1}	3.63	36.3	363
$\theta_e=1.0$	$\bar{\kappa}(H^-)$	5.57×10^{-2}	5.57×10^{-1}	5.57	55.7	557
	$\bar{\kappa}(H)$	0.02×10^{-2}
	$\bar{\kappa}$	5.59×10^{-2}	5.57×10^{-1}	5.57	55.7	557
$\theta_e=1.2$	$\bar{\kappa}(H^-)$	1.20×10^{-1}	1.20	12.0	120	1200
$\theta_e=1.4$	$\bar{\kappa}(H^-)$	2.33×10^{-1}	2.33	23.3	233	2330

We compare the observed intensity distribution in the emergent solar flux F_λ (obs.) with the flux $F_\lambda^{(1)}(0)$ to be expected in a gray atmosphere.¹⁴ It is evident that the *departures*,

$$\Delta \log F_\lambda = \log F_\lambda (\text{obs.}) - \log F_\lambda^{(1)}(0), \quad (7)$$

must be related more or less directly with the dependence of the continuous absorption coefficient κ'_v with wave length. Indeed, in the approximations leading to the temperature distribution (1) this relation must be one-one, since, with the adopted definition of $\bar{\kappa}$, the temperature distributions in the gray and the nongray atmospheres agree.¹⁵ This suggests that, with the known value of κ'_v due to H^- , we compare the predicted de-

¹³ G. Mülders, *Zs. f. Ap.*, 11, 132, 1935; G. Münch, *Ap. J.*, 102, 385, 1945; D. Chalonge and V. Kourganoff, *Ann. d'ap.* (in press).

¹⁴ The values of $F_\lambda^{(1)}(0)$ can be readily derived from the entries along the line $\tau = 0$ in Table 2 of "Radiative Equilibrium VII."

¹⁵ Cf. the remarks in italics on p. 343 in "Radiative Equilibrium VII."

partures from $F_\lambda^{(1)}(0)$ with those observed. The only uncertainty in these predictions will be of the nature of a "zero-point" correction, since a value of κ different from the one adopted will lead to an approximately constant additive correction to $\Delta \log F_\lambda$.¹⁶

In order, then, to make the comparison suggested in the preceding paragraph, we need to determine $\Delta \log F_\lambda$ in terms of κ'_λ due to H^- and an adopted κ . Assuming in the first instance that the contribution to κ is only H^- , we find that

$$a(H^-) = 5.62 \times 10^{-26} \text{ cm}^4/\text{dyne} \quad (8)$$

for an adopted value of

$$\theta_e = 0.8822. \quad (9)$$

The value of κ'_λ for $\theta = 0.8822$ can be found by simple interpolation in Table 7 of Chandrasekhar and Breen's paper. The ratios $\kappa'_\lambda/a(H^-)$ derived in this manner are

TABLE 3

THE PREDICTED DEPARTURES $[\log F_\lambda(\text{obs.}) - \log F_\lambda^{(1)}(0)]$ FROM GRAYNESS OF THE SOLAR ATMOSPHERE DUE TO THE ABSORPTION BY H^-

λA	$\frac{\kappa'_\lambda}{\bar{\kappa}(H^-)}$	$\frac{\kappa'_\lambda}{1.42\bar{\kappa}(H^-)}$	LOG F_λ (THEO.)		LOG $F_\lambda^{(1)}(0)$	$\Delta \text{LOG } F_\lambda$	
			$\bar{\kappa} = \bar{\kappa}(H^-)$	$\bar{\kappa} = 1.42\bar{\kappa}(H^-)$		$\bar{\kappa} = \bar{\kappa}(H^-)$	$\bar{\kappa} = 1.42\bar{\kappa}(H^-)$
			4000.....	0.686		0.483	14.489
4500.....	0.783	.551	14.468	14.390	+ .078
5000.....	0.881	.620	14.431	14.534	14.399	+ .032	+ .135
6000.....	1.029	.725	14.341	14.423	14.350	- .009	+ .073
7000.....	1.132	.797	14.259	14.329	14.285	- .026	+ .044
8000.....	1.188	.837	14.164	14.224	14.194	- .030	+ .030
9000.....	1.183	.833	14.070	14.128	14.098	- .028	+ .030
10,000.....	1.125	.792	13.982	14.034	13.999	- .017	+ .035
11,000.....	1.028	.724	13.897	13.946	13.901	- .004	+ .045
12,000.....	0.911	.642	13.817	13.862	13.805	+ .012	+ .057
13,000.....	0.788	.555	13.742	13.784	13.712	+ .030	+ .072
14,000.....	0.651	.458	13.674	13.713	13.624	+ .050	+ .089
15,000.....	0.523	.368	13.608	13.643	13.537	+ .071	+ .106
16,000.....	0.481	.339	13.532	13.566	13.454	+ .078	+ .112
17,000.....	0.486	.342	13.448	13.480	13.374	+ .074	+ .106
18,000.....	0.516	.363	13.362	13.395	13.297	+ .065	+ .098
19,000.....	0.562	.396	13.279	13.313	13.223	+ .056	+ .090
20,000.....	0.618	.435	13.197	13.230	13.152	+ .045	+ .078
21,000.....	0.679	.478	13.118	13.149	13.083	+ .035	+ .066
22,000.....	0.749	.527	13.042	13.073	13.016	+ .026	+ .057
23,000.....	0.820	0.577	12.971	13.003	13.952	+0.019	+0.051

given in Table 3 for various values of λ . With these values of $\kappa'_\lambda/a(H^-)$, the theoretical determination of $\Delta \log F_\lambda$ is straightforward with the help of the nomogram of Burkhardt's table,¹⁷ which one of us has recently published.¹⁸ The results of the determination are given in Table 3. In Figure 1 we have further compared the computed departures $\Delta \log F_\lambda$ with those observed.¹⁹ It is seen that the predicted variation of the

¹⁶ This is seen most directly in an approximation in which we expand the source function $B_\lambda(T)$ as a Taylor series about a suitable point and determine the emergent flux in terms of it (see, e.g., A. Unsöld, *Physik der Sternatmosphären*, p. 109, eq. [31.18], Berlin, 1938).

¹⁷ *Zs.f. Ap.*, 13, 56, 1936.

¹⁸ G. Münch, *Ap. J.*, 102, 385, Fig. 2, 1945.

¹⁹ For $\lambda > 9000 \text{ \AA}$ the observed departures were obtained from a reduction of the solar data by M. Minnaert, *B.A.N.*, 2, No. 51, 75, 1924; see also Unsöld, *op. cit.*, p. 32. For $\lambda < 9000 \text{ \AA}$ the reduction of G. Mülders (dissertation, Utrecht, 1934) was used.

departures runs remarkably parallel with the observed departures over the wavelength range 4000–20,000 Å. (The observational data do not seem specially reliable for $\lambda > 20,000$ Å.) However, the absolute values of the predicted departures are systematically less than the predicted departures by approximately a constant amount, indicating a zero-point correction in the sense that the adopted value of $\bar{\kappa}$ as due to H^- alone is somewhat too small. The calculations were accordingly repeated for other slightly larger values of $\bar{\kappa}$, and it was found that with $\bar{\kappa} = 1.42 \bar{\kappa}(H^-)$, the predicted and the observed departures agree entirely within the limits of the observational uncertainties over the whole region of the spectrum in which H^- contributes to the absorption. The

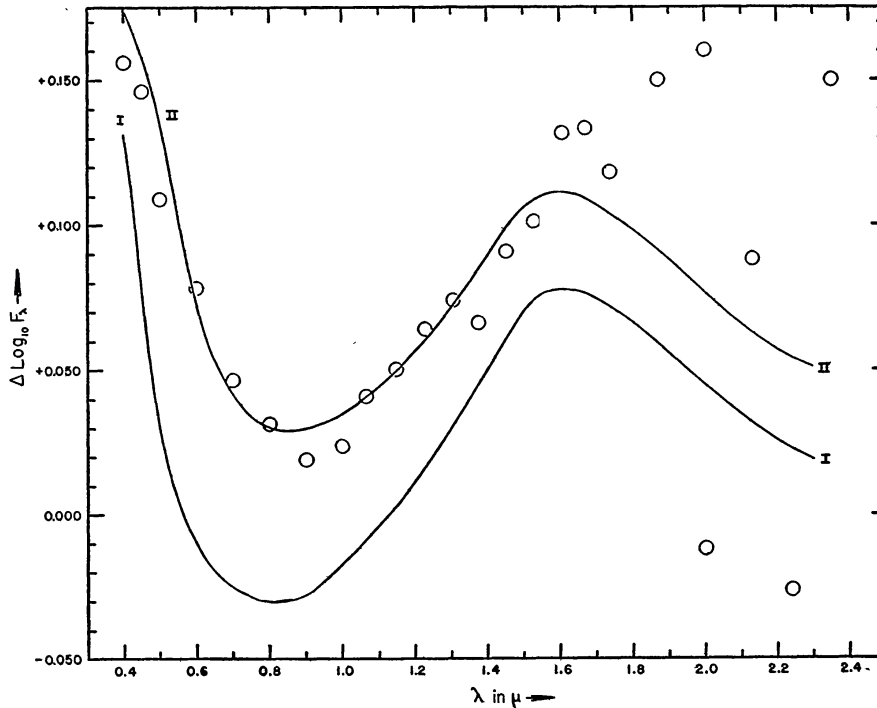


FIG. 1.—Comparison of the observed and the theoretically predicted departures [$\log F_\lambda - \log F_\lambda^1(0)$] from a gray atmosphere due to the absorption by H^- . The circles represent the observed departures of the solar emergent flux from that of a gray atmosphere, while Curves I and II are the theoretically derived departures on the two assumptions $\bar{\kappa} = \bar{\kappa}(H^-)$ and $\bar{\kappa} = 1.42 \bar{\kappa}(H^-)$.

agreement is, in fact, so striking that we may say that H^- reveals its presence in the solar atmosphere by its absorption spectrum.

We may finally remark on the value of $\bar{\kappa} = 1.42 \bar{\kappa}(H^-)$, indicated by the comparisons we have just made: it can, in fact, be deduced empirically from the solar data on the continuous spectrum that the absorption in the violet ($\lambda < 4000$ Å) must increase the value of κ derived from the visible and the infrared regions of the spectrum by a factor of the order of 1.5.²⁰

4. *The predicted color-effective temperature relations: comparison with observations.*—All earlier attempts²¹ to predict the color temperatures in the region $\lambda\lambda$ 4000–6500 Å for stars of spectral types A0–G0 in agreement with the observations have failed. This failure in the past has been due to the following circumstance: The observed relation between the color and the effective temperatures and, in particular, the fact that $T_c > T_e$

²⁰ Cf. G. Münch, *Ap. J.*, 102, 385, 1945, esp. the remarks preceding eq. (19) on p. 394.

²¹ R. Wildt, *Ap. J.*, 93, 47, 1941, and *Observatory*, 64, 195, 1942; R. E. Williamson, *Ap. J.*, 97, 51, 1943.

implies that the continuous absorption coefficient is an increasing function of λ in the spectral region observed. But the physical theory on which the calculations were made placed the maximum of the absorption-curve in the region of λ 4500 Å; this was incompatible with the observations and, moreover, predicted color temperatures less than the effective temperatures, contrary to all evidence. Indeed, on the strength of this discrepancy, it was concluded that H^- as a source of absorption was inadequate even in the region λ 4500–6500 Å, and the existence of an unknown source operative in this region was further inferred. However, later evaluations²² of the bound-free transitions of H^- showed the unreliability of earlier determinations and placed the maximum of the absorption-curve in the neighborhood of λ 8500 Å. The addition of the free-free transitions pushes this maximum only still further to the red. It is therefore evident that on the revised physical theory we should be able to remove the major discrepancies of the subject. We shall now show how complete the resolution of these past difficulties is.

From the point of view of establishing the adequacy of the physical theory in the region λ 4000–6500 Å, it is most instructive to consider the theoretical predictions for color temperatures which can be directly compared with the color determinations at Greenwich,³ for the Greenwich measures are based on the mean gradients in the wavelength interval 4100–6500 Å, and it is in the prediction of these colors that the earlier calculations were most discordant.²³

Now, from the Planck formula in the form

$$i_\lambda = \frac{2hc^2}{\lambda^5} \frac{1}{e^{c_2/\lambda T} - 1}, \quad (10)$$

it readily follows that

$$\frac{1}{i_\lambda} \frac{di_\lambda}{d(1/\lambda)} = 5\lambda - \frac{c_2}{T} (1 - e^{-c_2/\lambda T})^{-1}. \quad (11)$$

Defining the gradient

$$\phi = \frac{c_2}{T} (1 - e^{-c_2/\lambda T})^{-1} \quad (12)$$

in the usual manner, we can write

$$\frac{1}{M} \frac{d \log_{10} i_\lambda}{d(1/\lambda)} = 5\lambda - \phi \quad \left(\frac{1}{M} = 2.303 \right). \quad (13)$$

If F_{λ_1} and F_{λ_2} are the emergent fluxes at two wave lengths λ_1 and λ_2 and if ϕ is the mean gradient in this wave-length interval, then we can write, in accordance with equation (13)

$$\phi = 5\lambda_m - \frac{1}{M} \frac{\log_{10} (F_{\lambda_1}/F_{\lambda_2})}{\lambda_1^{-1} - \lambda_2^{-1}}, \quad (14)$$

where λ_m denotes an appropriate mean wave length for the interval to which the gradient ϕ refers. Equation (14) can be re-written in the following form:

$$\phi = 5\lambda_m - \frac{1}{M} \frac{\Delta \log_{10} F}{\Delta (1/\lambda)}. \quad (15)$$

According to equation (15), the theoretical determination of color temperatures will proceed by determining, first, the gradient ϕ from the values of F_λ at the end-points of the wave-length interval and then determining the temperature which will give this gradient.

²² S. Chandrasekhar, *Ap. J.*, **102**, 223, 395, 1945

²³ Cf. Fig. 6 in Williamson's paper (*op. cit.*).

For the Greenwich measures $\lambda_m = 0.55 \mu$, and equation (15) becomes

$$\phi (\text{Greenwich}) = 2.75 - 2.56 \log_{10} \left(\frac{F_{4100}}{F_{6500}} \right), \quad (16)$$

provided that, in determining the gradients, wave lengths are measured in microns.²⁴

In Table 4 we have listed the values of $\kappa'_\lambda/\bar{\kappa}$ for the wave lengths 4100 Å and 6500 Å for various values of θ_e and p_e . In terms of these values the determination of the fluxes at the two wave lengths 4100 Å and 6500 Å is straightforward with the help of Burkhardt's table. The gradient ϕ then follows according to equation (16) and, from that, the color temperature. The reciprocal color temperatures $\theta_c = 5040/T_c$ derived in this manner are given in Table 5. The resulting color-effective temperature relations are illustrated

TABLE 4
 $\kappa'_\lambda/\bar{\kappa}$ IN MODEL STELLAR ATMOSPHERES

$5040/T_e$	$\lambda \text{Å}$	$p_e=10$	$p_e=10^2$	$p_e=10^3$	$p_e=10^4$
$\theta=0.5$	λ 3647	{.....	3.45	3.22	2.68
		{.....	0.161	0.181	0.332
	λ 4000	0.210	0.212	0.238	0.397
	λ 4600	0.316	0.318	0.346	0.513
	λ 6500	0.826	0.834	0.848	0.991
$\theta=0.6$	λ 8203	{.....	1.51	1.51	1.55
		{.....	0.490	0.526	0.788
	λ 3647	{.....	4.04	2.60	1.09
		{.....	0.178	0.427	0.685
	λ 4000	0.148	0.205	0.481	0.770
$\theta=0.7$	λ 4600	0.221	0.278	0.585	0.901
	λ 6500	0.579	0.637	0.935	1.25
	λ 8203	{.....	1.27	1.36	1.45
		{.....	0.424	0.885	1.36
	λ 3647	{6.06	2.82	0.961	0.684
$\theta=0.8$		{0.176	0.461	0.625	0.645
	λ 4000	0.208	0.521	0.695	0.725
	λ 4600	0.276	0.617	0.810	0.848
	λ 6500	0.546	0.901	1.11	1.14
	λ 8203	{0.889	1.105	1.22	1.24
$\theta=0.9$		{0.356	0.893	1.19	
	λ 3647	{1.54	0.720	0.625
		{0.518	0.601	0.614	0.611
	λ 4000	0.582	0.671	0.685	0.685
	λ 4600	0.681	0.781	0.800	0.800
$\theta=0.9$	λ 6500	0.961	1.06	1.09	1.09
	λ 8203	{1.11	1.178}	1.19	1.19
		{1.01	1.164}		
	λ 3647	{0.708	0.642	0.636	0.636
		{0.631	0.636	0.690	0.690
$\theta=0.9$	λ 4000	0.690	0.690	0.800	0.800
	λ 4600	0.800	0.800	0.800	0.800
	λ 6500	1.09	1.09	1.09	1.09
	λ 8203	{1.16	1.16	1.16	1.16
		{.....

²⁴The constant c_2 in eq. (12) then has the value 14,320.

in Figure 2. For comparison we have also plotted in this figure the Greenwich determinations for stars on the main sequence and of spectral types A0–G0 (reduced, however, to the Morgan, Keenan, and Kellman system of spectral classification). The color temperature of the sun for this wave-length interval is also plotted in Figure 1. It is seen from Figure 1 that the agreement between the observed and the theoretical color temperatures is entirely satisfactory, particularly when it is remembered that the earlier calculations failed even to predict the correct sign for $\theta_c - \theta_e$. It will, however, be noted that the observed values of θ_e for spectral types later than F0 are somewhat larger than the pre-

TABLE 5
THEORETICAL RECIPROCAL COLOR TEMPERATURES AND THE PREDICTED DISCONTINUITIES AT THE HEAD OF THE BALMER AND THE PASCHEN SERIES*

p_e	θ_e					
	0.5	0.6	0.7	0.8	0.9	1.0
10 ¹ { $\theta_e(G)$ $\theta_e(B \text{ and } C)$ D_B				0.68 .61 .31	0.80 .69 .015	0.88 .75
10 ² { $\theta_e(G)$ $\theta_e(B \text{ and } C)$ D_B D_P		0.45	0.60 .47 [.50] .030	.73 .63 .07 .001	.80 .69	.88 .75
10 ³ { $\theta_e(G)$ $\theta_e(B \text{ and } C)$ D_B D_P	[0.31]	.52 .42 [.34] .051	.65 .56 .13 .003	.74 .64	.80 .69	.88 .75
10 ⁴ { $\theta_e(G)$ $\theta_e(B \text{ and } C)$ D_B D_P	[.39] [.34] [.40] [.071]	.59 .50 .12 .006	.66 .58 .018	.74 .64	.80 .69	.88 .75
Pure { $\theta_e(G)$ H^- { $\theta_e(B \text{ and } C)$.52 0.41	.59 0.50	.66 0.58	.74 0.64	.80 0.69	.88 0.75

* $\theta_e(G)$ and $\theta_e(B \text{ and } C)$ are the reciprocal color temperatures, $5040/T_e$, appropriate for the wave-length intervals 4100–6500 Å and 4000–4600 Å, respectively; D_B and D_P , representing the logarithm of the ratio of the fluxes at the two sides of the series limits, are the expected Balmer and Paschen discontinuities, respectively.

dicted values, though the agreement is as good as can be expected in the case of the sun. The reason for this must undoubtedly be the crowding of the absorption lines toward the violet in the later spectral types and the consequent depression of the continuous spectrum in this region. The correctness of this explanation is apparent when it is noted that in the case of the sun, in which allowance has been made for this effect of the lines on the continuum, the discordance is not present.

Comparisons similar to those we have just made also can be made with the measurements of Barbier and Chalonge⁴ on the color temperatures based on the observed gradients in the wave-length interval 4000–4600 Å. The formula giving the theoretical gradient for this wave-length interval takes the form

$$\phi(B \text{ and } C) = 2.175 - 7.06 \log_{10} \left(\frac{F_{4000}}{F_{4600}} \right). \quad (17)$$

The values of $\kappa'_\lambda/\bar{\kappa}$ at λ 4000 Å and λ 4600 Å are given in Table 4, and the reciprocal color temperatures derived from these in Table 5. The results are further illustrated in Figure 3, where the theoretical relations for various electron pressures are compared with the measures of Barbier and Chalonge (reduced also to the Morgan, Keenan, and Kellman system of spectral classification). It is seen that the general agreement is again good, though there are now somewhat larger differences between the computed and the observed color temperatures for spectral types later than F0 than were encountered in the comparison with the Greenwich colors. This must again be due to the crowding of the absorption lines toward the violet in the later spectral types and the further fact that

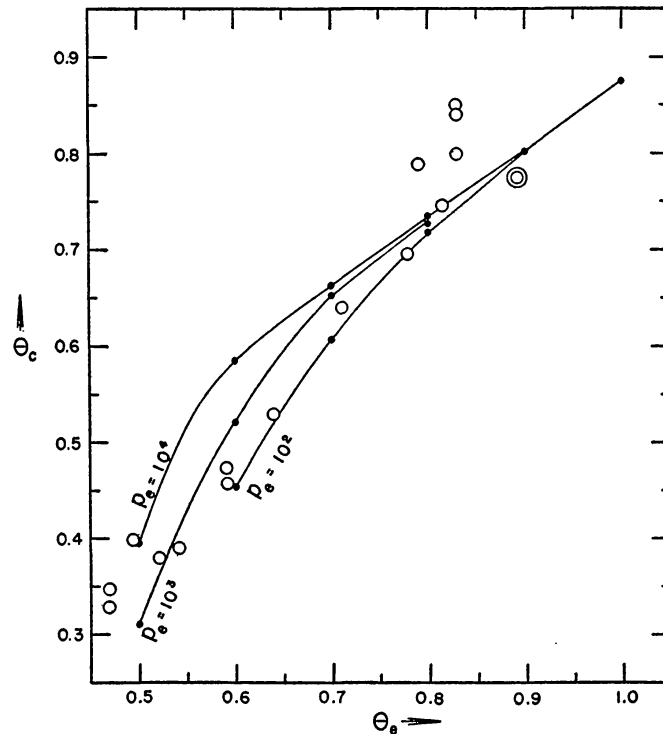


FIG. 2.—Comparison of the observed and the theoretical color effective-temperature relations for the wave-length interval 4100–6500 Å. The ordinates denote the reciprocal color temperatures and the abscissae denote the reciprocal effective temperatures ($\theta = 5040/T$). The circles represent the Greenwich color determinations reduced to the Morgan, Keenan, and Kellman system of spectral classification. The double circle represents the sun.

the base line for the Barbier and Chalonge colors is much shorter than that for the Greenwich colors.

5. *The discontinuities at the head of the Balmer and the Paschen series.*—With the physical theory of the continuous absorption coefficient now available, we can also predict the extent of the discontinuities which we may expect at the head of the Balmer and the Paschen series of hydrogen. For this purpose the values of $\kappa'_\lambda/\bar{\kappa}$ on the two sides of the series limits are also given in Table 4. From these values it is a simple matter to estimate the discontinuities which will exist at the head of the Balmer and the Paschen series, and they are given in Table 5. The results for the Balmer discontinuities are further illustrated in Figure 4, in which the discontinuities measured by Barbier and Chalonge⁴ for various stars are also plotted. The progressive increase of the electron pressure as we go from the later to the earlier spectral types is particularly apparent

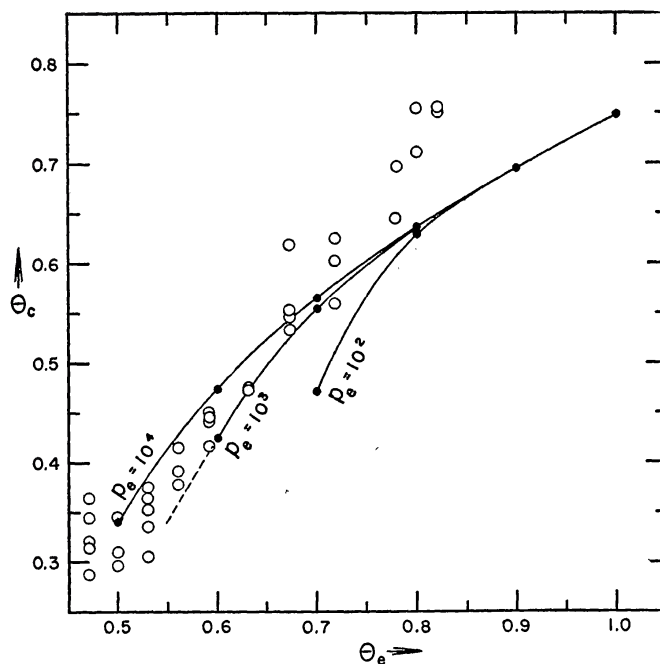


FIG. 3.—Comparison of the observed and the theoretical color effective-temperature relations for the wave-length interval 4000–4600 Å. The ordinates denote the reciprocal color temperatures, and the abscissae denote the reciprocal effective temperatures $\theta = 5040/T$. The circles represent the color determinations of Barbier and Chalange for the wave-length interval 4000–4600 Å, reduced to the Morgan, Keenan, and Kellman system of spectral classification.

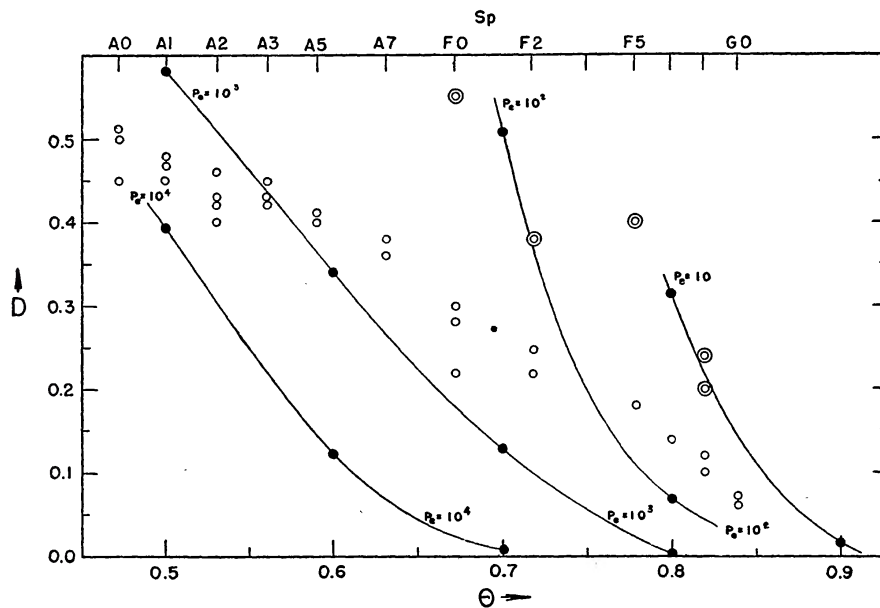


FIG. 4.—The predicted discontinuities (D) at the head of the Balmer series for various effective temperatures and electron pressures. The circles represent the discontinuities as measured by Barbier and Chalange. (The double circles represent the observations for supergiants.)

from Figure 4; this progression is, moreover, in agreement with what is indicated by the color determinations (cf. Figs. 2 and 3). In Table 6 we give the electron pressures for the main-sequence stars of various spectral types estimated in this manner.

6. *Concluding remarks.*—While our discussion in the preceding sections has established the unique role which H^- plays in determining the character of the continuous spectrum of the sun and the stars, it should not be concluded that the various other

TABLE 6
ELECTRON PRESSURES FOR STARS ON THE MAIN SEQUENCE

Type	$\log p_e$	Type	$\log p_e$	Type	$\log p_e$
A1.....	3.7	F0.....	2.4	F8.....	1.4
A2.....	3.3	F2.....	2.2	G0.....	1.2
A3.....	3.0	F4.....	2.0	G2.....	1.0
A5.....	2.8	F5.....	1.8		
A7.....	2.6	F6.....	1.6		

astrophysical elements of the theory are equally well established. Indeed, the theory of model stellar atmospheres as developed by Strömgen in recent years must not only be revised on the basis of the new absorption coefficients of H^- but also be advanced still further before we can be said to have a completely satisfactory account of all the classical problems of the theory of stellar atmospheres. But our discussion in this paper does give us the confidence that the continuous absorption by H^- discovered by Wildt must provide the key to the solution of many of these problems.